Materials Science in Semiconductor Processing 19 (2014) 107–113

Contents lists available at ScienceDirect

Materials Science in Semiconductor Processing

journal homepage: www.elsevier.com/locate/mssp

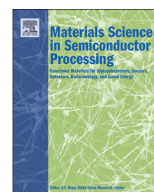

Structural and the optical dispersion parameters of nano-CdTe thin film/flexible substrate

E.R. Shaaban [a,*], I.S. Yahia [b,c], N. Afify [d], G.F. Salem [e], W. Dobrowolski [f]

[a] Department of Physics, Faculty of Science, Al-Azahar University, Assiut 71542, Egypt
[b] Department of Physics, Faculty of Science, King Khalid University, P.O. Box 9004, Abha, Saudi Arabia
[c] Nano-Science & Semiconductor Labs, Department of Physics, Faculty of Education, Ain Shams University, Roxy, Cairo, Egypt
[d] Physics Department, Faculty of Science, Assiut University, Assiut, Egypt
[e] Thin Film Laboratory, Department of Physics, Faculty of Education, Ain Shams University, Roxy, Cairo, Egypt
[f] Institute of Physics, Polish Academy of Sciences, Al. Lotnikow, 32/46, 02-668 Warszawa, Poland

ARTICLE INFO

Available online 28 December 2013

Keywords:
CdTe
Thin film
XRD
Optical constants
Optical bandgap

ABSTRACT

CdTe thin films of different thicknesses were deposited on polymer substrates for flexible optical devices applications. X-ray diffractogram of different thicknesses for CdTe films are measured and their patterns exhibit polycrystalline nature with a preferential orientation along the (111) plane. The optical constants of CdTe films were calculated based on the measured transmittance spectral data using Swanepoel's method in the wavelength range 400–2500 nm. The refractive index *n* and absorption index *k* were calculated and the refractive index exhibits a normal dispersion. The refractive index dispersion data followed the Wemple–DiDomenico model based on single oscillator. The oscillator dispersion parameters and the refractive index no. at zero photon energy were determined. The possible optical transition in these films is found to be allowed direct transition with energy gap increase from 1.46 to 1.60 eV with the increase in the film thickness. CdTe/flexible substrates are good candidates in optoelectronic devices

© 2013 Elsevier Ltd. All rights reserved.

1. Introduction

Cadmium telluride is considered at present one of the most promising materials, for device applications. It has a high absorption coefficient in the visible range of the solar spectrum and its band gap is close to the optimum value for efficient solar energy conversion [1,2]. CdTe/CdS solar cells are one of the prospective candidates for widespread commercial success in solar energy conversion [3–6]. They can be produced at low price with good efficiency and excellent stability. Thin film polycrystalline photovoltaics have been aimed at the lower cost market where lower efficiency is acceptable [7,8]. The conventional cells are usually manufactured on glass substrates and offer no weight advantage over single crystal cells. Producing thin film cells on thin foil substrates (0.05 mm or less thick), however, offers several advantages for space as well as terrestrial applications. Since the substrate material can be as thin as 0.05 mm, the weight savings are significant in the case of thin film devices on flexible substrates. Furthermore, the photovoltaic devices on flexible substrates can be folded in any shape, and the supporting structure requirements are minimum compared to the heavy glass substrates. One of the major obstacles in the development of low cost and high efficiency solar cells is the use of glass substrates. The poor thermal conductivity of glass makes it extremely difficult to maintain a constant annealing temperature across a large area panel and to avoid thermal stresses which cause breakage during fabrication. Thus, panel efficiency is much lower than would be expected from the efficiency of small devices. Hence metal foil mounted cells can both reduce weight and promise efficient cheaper cells.

* Corresponding author. Tel.: +20 1093344297; fax: +20 88181436.
E-mail addresses: esamramadan2008@yahoo.com, esam_ramadan2008@yahoo.com (E.R. Shaaban).

1369-8001/$ - see front matter © 2013 Elsevier Ltd. All rights reserved.
http://dx.doi.org/10.1016/j.mssp.2013.12.013

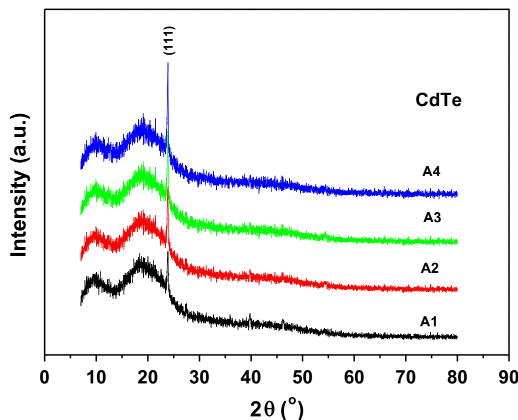

Fig. 1. The XRD patterns of CdTe films/flexible substrates of different thicknesses.

High efficiency can be achieved due to the high optical absorption coefficient. For example, in CdTe, light is absorbed within 2 mm and crystalline defects are relatively less important than in single crystal cells. Since the cells are so thin actual damage per unit radiation flux is less. Hence, thin film solar cells should be less susceptible to radiation degradation than single crystal solar cells. The interest in CdTe-based devices on light weight and flexible substrates gained interest in mid-90s and there are large number of reports on the film growth [9–24], post deposition treatments [10–12], structural characterization [19–24] and optoelectronic characterization [25–31]. We can concluded that CdTe thin film on flexible substrates still requires more studies to optimize its optical and electrical characterizations for high efficiency solar cell absorbed materials. The thermal conductivity and melting point T_m of utilized flexible substrate (polymer acetate sheet) is 0.16–0.36 W m^{-1} K^{-1} [32] and 564 K [33] respectively.

In the present work, CdTe/flexible polymer substrates were prepared and characterized by XRD and optical spectroscopy measurements. XRD parameters such as crystallite size, microstrain were calculated and interpreted as a function of film thickness. Optical constants were calculated on the basis of Swanepoel's method for the first time. The relation between the structure of the studied CdTe thin films and their optical constants parameters were described in details. Optical dispersion parameters were calculated and interpreted.

2. Experimental techniques

CdTe single crystal was grown by the Bridgman technique in the Institute of Physics, Warsaw, Poland. Different thickness of CdTe thin films were deposited by thermal evaporation from a resistance heating quartz glass crucible onto transparent polymer acetate sheets as flexible substrates using high vacuum coating unit type Edward 306 A. Film thicknesses and the rate of evaporation were monitored with a quartz crystal monitor FTM4 attached to the vacuum system. Films were grown at a pressure of 10^{-6} Pa. The mechanical rotation of the substrate holder ($\approx$30 rpm) during deposition produced homogeneous film. The distance between the source heater and substrates holder is 21 cm to avoid any heat flow from the source to the substrates.

The elemental composition of the films was analyzed by an energy dispersive X-ray spectrometer (EDXS) unit interfaced to scanning electron microscope (SEM) (Philips XL) operating at an accelerating voltage of 30 kV. The relative error of determining the indicated elements does not exceed 3.2%. The structure of the as-deposited films were measured at room temperature by an analytical X′Pert Diffractometer System, which has CuK_α as a radiation source of wavelength λ=1.540598 Å. The X-ray tube voltage and current were 40 kV and 30 mA, respectively. The 2θ range is 4–80° with a step size of 0.02 and scanning time of 0.4 second.

The transmittance $T(\lambda)$ and reflectance $R(\lambda)$ spectra of the as-deposited CdTe thin films of different thicknesses were measured at normal incidence of light in the spectral range of 400–2600 nm using a double-beam spectrophotometer (JASCO model V-670 UV–vis–NIR).

3. Results and discussion

3.1. X-ray diffraction analysis

The thickness of the four CdTe thin films deposited on flexible substrates as calculated in terms of Swanepoel's method was found to be 701 nm, 1052 nm, 1328 nm and 1691 nm. Effect of the change in thickness of the film on the structural using the X-ray diffractogram are shown in Fig. 1. XRD patterns exhibit polycrystalline nature and a major diffraction peak is observed at 2θ=23.80° along with few weak peaks. The presence of the predominant peak at 2θ=23.80° suggests that the CdTe films are of zinc blende (cubic) structure (JCPDS Data file: 1-75-2086-cubic) with lattice parameters $a=b=c$=6.41 Å and a preferential orientation along the (111) plane. The (111) direction is the close-packing direction of the zinc blende (cubic) structure and this type of textured growth has often been observed in polycrystalline CdTe films grown on the flexible substrate. It can be seen that the film thickness affects the XRD pattern of CdTe thin films i.e. the peak intensity increases with increasing film thickness. Each X-ray diffraction line profile obtained in a diffractometer is broadened due to instrumental and physical factors (crystallite size and lattice strains). The microstructure parameters of the CdTe films such as crystallites size (D_v) and microstrain (e) were calculated by analyzing the XRD data using the Scherrer's formula

$$D=\frac{0.9\lambda}{\beta \cos \theta}, \quad (1)$$

and Wilson formula

$$e=\frac{\beta}{4 \tan \theta}, \quad (2)$$

where β describes the structural broadening, which is the difference in integral X-ray peak profile width between the sample and a standard (silicon) and is given by$\beta=\sqrt{\beta_{obs}^2-\beta_{std}^2}$. Table 2 shows a comparative look of microstructure parameters (D_v and e) of the CdTe films of

Table 1
Values of λ, T_M and T_m for the four different thicknesses of polycrystalline CdTe thin films of corresponding to transmission spectra of Fig. 1; the calculated values of refractive index and film thickness are based on the envelope method.

Sample	λ	T_M	T_m	s	n_1	d_1(nm)	m_0	m	d_2(nm)	n_2
A1										
	1134	0.796	0.535	1.378	2.441	–	2.923	3	696.8	2.428
	1304	0.823	0.568	1.374	2.354	701.2	2.451	2.5	692.5	2.327
	1570	0.86	0.609	1.365	2.261	656.7	1.955	2	694.5	2.241
	2018	0.892	0.67	1.357	2.106	–	1.417	1.5	718.6	2.16
	$\bar{d}_2 = $ **701 nm, σ_2=12.1 nm (1.7%)**									
A2										
	1074	0.744	0.493	1.379	2.524	–	5.122	5	1064	2.552
	1162	0.764	0.515	1.377	2.465	1101	4.624	4.5	1061	2.485
	1272	0.789	0.538	1.375	2.412	1112	4.132	4	1055	2.418
	1412	0.813	0.561	1.370	2.36	1092	3.644	3.5	1047	2.349
	1604	0.836	0.584	1.363	2.306	1055	3.134	3	1043	2.287
	1878	0.856	0.608	1.357	2.249	–	2.61	2.5	1044	2.231
	$\bar{d}_1 = $ **1090 nm, σ_1=25 nm (2.3%),** $\bar{d}_2 = $ **1052 nm, σ_2=9 nm (0.86%)**									
A3										
	1072	0.72	0.467	1.379	2.603	–	6.613	6.5	1338	2.624
	1140	0.734	0.482	1.378	2.555	1361	6.103	6	1339	2.575
	1214	0.746	0.498	1.376	2.502	1386	5.612	5.5	1334	2.514
	1306	0.763	0.516	1.374	2.456	1382	5.121	5	1330	2.459
	1422	0.784	0.533	1.37	2.416	1360	4.627	4.5	1324	2.409
	1570	0.804	0.552	1.365	2.375	1337	4.119	4	1322	2.365
	1760	0.824	0.570	1.359	2.332	1344	3.609	3.5	1321	2.319
	2012	0.841	0.588	1.357	2.295	–	3.106	3	1315	2.273
	$\bar{d}_1 = $ **1361 nm, σ_1=19.6 nm (1.4%),** $\bar{d}_2 = $ **1328 nm, σ_2=8.7 nm (0.66%)**									
A4										
	1178	0.716	0.466	1.377	2.597	–	7.59	7.5	1701	2.612
	1242	0.729	0.478	1.375	2.559	1722	7.096	7	1698	2.571
	1318	0.741	0.491	1.373	2.522	1760	6.59	6.5	1698	2.533
	1402	0.755	0.503	1.37	2.491	1766	6.118	6	1689	2.487
	1506	0.769	0.517	1.367	2.456	1706	5.615	5.5	1686	2.449
	1630	0.782	0.53	1.363	2.418	1686	5.108	5	1685	2.41
	1784	0.795	0.544	1.358	2.38	1691	4.594	4.5	1686	2.374
	1976	0.807	0.558	1.356	2.347	–	4.09	4	1684	2.337
	$\bar{d}_1 = $ **1721 nm, σ_1=34.3 nm (2%),** $\bar{d}_2 = $ **1691 nm, σ_2=7 nm (0.4%)**									

Table 2
The dispersion energy E_d, the single-oscillator energy E_o refractive index $n(o)$ at $(E \to 0)$ and energy gap E_g^{opt} of different thickness of CdTe thin films.

Sample	Thickness (nm)	FWHM	Crystallitze size (nm)	Micro-stain	E_d (eV)	E_o (eV)	$n(o)$	E_g^{opt} (eV)
A1	701	0.37	24.8	0.02275	4.14	2.94	1.55	1.46
A2	1052	0.35	26.2	0.02152	4.19	3.01	1.55	1.51
A3	1328	0.30	30.6	0.01845	4.41	3.09	1.56	1.56
A4	1691	0.26	35.3	0.01599	5.66	3.19	1.67	1.60

different thicknesses on flexible substrate. It is observed that the crystallite size increases with the increasing of the film thickness. The microstrain decreases with the increase of the film thickness as shown in Table 2. Such a decrease in micro-strain reflects the decrease in the concentration of lattice imperfections, which might be attributed to the decrease of breadth with the increasing film thickness [26]. The crystallize size ranging from 25 to 35 nm in the present study is lower than those reported by Shaaban et. al. [34], which exhibit the crystallite size in the range of 54–68 nm. Such low values of crystallize size might be attributed to the flexible substrate which increases the broadening of the peaks [35], which causes the reduction of crystallite size according to Scherrer′s formula.

3.2. Optical constants of CdTe/flexible substrate.

The transmittance spectra of the deposited films as a function of wavelength are depicted in Fig. 2. It can be seen that the non-shrinking interference fringes (fringes of equal chromatic order FECO) observed in transmittance spectra at longer wavelength (1000–2000 nm) indicate the homogeneity and smoothness of the deposited films. After a wavelength greater than 2000 nm small oscillations

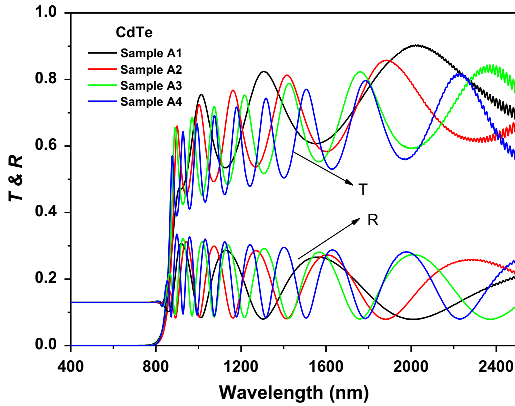

Fig. 2. The measured transmittance and reflectance spectra of CdTe films/flexible substrates of different thicknesses.

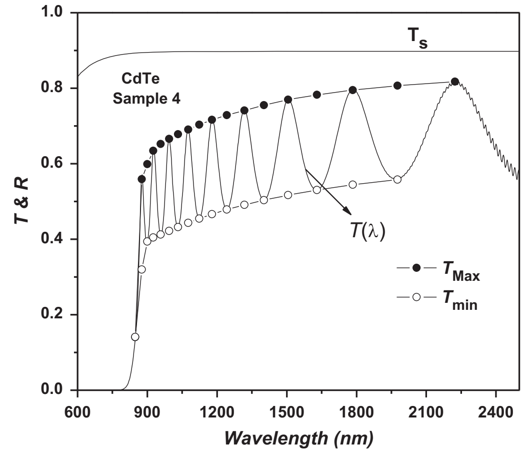

Fig. 3. The transmittance spectra according to Swanepole′s method of CdTe/flexible substrates of thickness.

occur and its amplitude increases with increasing the wavelength. The increase in amplitude of oscillation with the wavelength greater than 2000 nm may be attributed to the inter-diffusion of the CdTe film and the flexible substrate due to the thermal energy of IR incident light.

Furthermore, the absorption edge (beginning of absorption process within the film materials) of the deposited films show blue shift as the increasing the film thickness. The reason for the blue shift may be complex. However, as the particle size of the films is below 100 nm, quantum size effect can be used to explain the magnitude of the shift. Quantum size effect can be expressed by the Brus equation [36]

$$\Delta E = \frac{\eta\pi^2}{2R^2}\left[\frac{1}{m_e}+\frac{1}{m_h}\right]-\frac{1.786e^2}{\varepsilon R}-0.248E_{Ry} \tag{3}$$

where η is the converting efficiency of quantum, R is the radius of the particle, m_e and m_h are the effective masses for the electrons and holes, respectively, ε is the dielectric constant, and Ry is effective Rydberg energy. The first item is bondage energy, which is proportionate to$1/R^2$; the second item is the coulomb attraction of electrons and holes, and the third item represents the space amendatory effect. As the particle size reduces, because the increase of bondage energy is more evident than the coulomb item that leads to the decrease of energy, so smaller grain size leads to a larger shift of the absorption edge. This shift is a direct consequence of the thickness dependence of the optical transmittance spectra and consequently optical band gap of the deposited films.

The envelope method suggested by Swanepoel [35], employed extensively by many researchers[37–40], was used to calculate the refractive index and thickness of the thin films. Swanepoel′s method is based on a creation of top and bottom envelopes to the interference maxima and minima observed in transmittance spectra. A first approximate value of the refractive index of the film n_1, in the spectral region of medium and weak absorption, can be calculated by the expression

$$n_1 = [N_1 + (N_1^2 - s^2)^{1/2}]^{1/2} \tag{4}$$

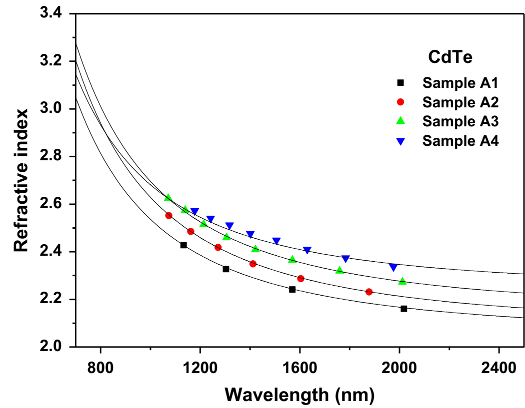

Fig. 4. The refractive index as a function of wavelengths of CdTe films/flexible substrates of different thicknesses.

where

$$N_1 = 2s\frac{T_M - T_m}{T_M T_m} + \frac{s^2+1}{2}$$

Here T_M and T_m, are the transmission maximum and the corresponding minimum at a certain wavelength λ. Alternatively, one of these values is an experimental interference extreme and the other one is derived from the corresponding envelope; both envelopes were computer-generated using the origin version 7 program using more than one procedure. On the other hand, the necessary values of the refractive index of the substrate are obtained from the transmission spectrum of the substrate, T_s using the well-known equation

$$s = \frac{1}{T_s} + \left(\frac{1}{T_s} - 1\right)^{1/2} \tag{5}$$

The values of the refractive index n, as calculated from Eq. (2) are shown in Table 1. The accuracy of this initial estimation of the refractive index is improved after calculating d, as will be explained below. Now, it is necessary to take into account the basic equation for interference

fringes

$$2nd = m\lambda \tag{6}$$

where the order numbers m is integer for maxima and half integer for minima. Moreover, if n_{e1} and n_{e2} are the refractive indices at two adjacent maxima (or minima) at λ_1 and λ_2, it follows that the film thickness is given by the expression

$$d = \frac{\lambda_1 \lambda_2}{2(\lambda_1 n_{e2} - \lambda_2 n_{e1})} \tag{7}$$

The values of d of different samples determined by this equation, are listed as d_1, in Table 1. The average value of d_1, (ignoring the last two values). This value can now be used, along with n_1, to calculate the "order number" m_0 for the different extremes using Eq. (6). The accuracy of d can now be significantly increased by taking the corresponding exact integer or half integer values of m associated to each extreme (Fig. 3) and deriving a new thickness, d_2 from Eq. (4), again using the values of n_1, the values of d found in this way have a smaller dispersion ($\sigma_1 > \sigma_2$). It should be emphasized that the accuracy of the final thickness is better than 1%. (Table 1). With the exact value of m and the very accurate value of Eq. (4) can then be solved for n at each λ and, thus, the final values of the refractive index n_2 are obtained (Table 1). Fig. 4 illustrates the dependence of refractive index n as a function of wavelength for different thickness of CdTe thin films. Now, the values of n can be fitted to a reasonable dispersion function such as the two-term Cauchy function, $n(\lambda) = a + b/\lambda^2$, which can be used for extrapolation the whole wavelength dependence of refractive index, see Fig. 4 [36,40]. The least squares fit of the four sets of values of n corresponding the four different composition samples, yields $n = 2.044 + 4.93 \times 10^5/\lambda^2$ for A1, $n = 2.075 + 5.54 \times 10^5/\lambda^2$ for A2, $n = 2.137 + 5.59 \times 10^5/\lambda^2$ for A3 and $n = 2.235 + 4.47 \times 10^5/\lambda^2$ for A4, respectively. As clearly seen in Fig. 4 the change in the n values is related to the change in the film thickness, i.e. the refractive index values increase with increasing the film thickness of CdTe thin film. The increase in refractive index with increasing film thickness may be attributed to the increased density of the film and increasing in crystallites size.

The spectral dependence data of the refractive index dispersion of the as deposited different thickness of CdTe thin films can be evaluated according to the single-effective-oscillator model proposed by Wemple–DiDomenico (WDD) model [41]. The model suggests that the refractive index, n, of the films could be correlated to the oscillator energy, E_O and the dispersion energy, E_d, by the following formula:

$$n^2 - 1 = \frac{E_o E_d}{E_o^2 - (h\upsilon)^2} \tag{8}$$

where $(h\upsilon)$ is the photon energy and E_o, E_d are single-oscillator constants. As shown in Fig. 5, the optical dispersion behavior, $(n^2-1)^{-1}$ against $(h\upsilon)^2$ of the investigated nanocrystalline CdTe thin films with different thickness. The oscillator parameters E_o and E_d were determined by fitting a straight line to the points. The slope of the linear relationship represents the $(E_o E_d)^{-1}$ and intercept with the vertical axis equal to (E_o/E_d). The values obtained of dispersion parameters E_o and E_d for the as-deposited of

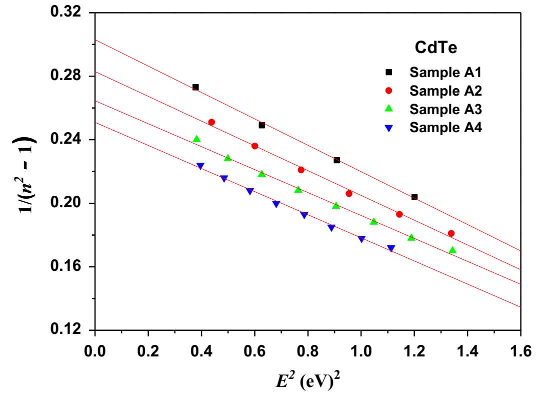

Fig. 5. Plotting of $(n^2-1)^{-1}$ as a function of E^2 of CdTe films/flexible substrates of different thicknesses.

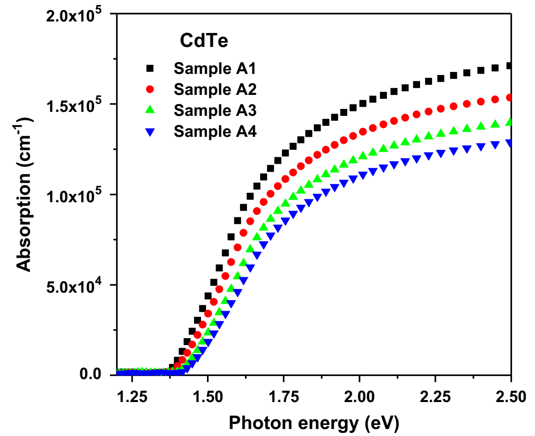

Fig. 6. Plotting of absorption as a function of photon energy of CdTe films/flexible substrates of different thicknesses.

different thickness of CdTe thin films are listed in Table 2. The refractive index n_o at zero photon energy, which is defined by the infinite wavelength dielectric constant as: $\varepsilon_\infty^{WD} = n_o^2$ where $n_o^2 = 1 + E_d/E_o$. The calculated values of n_o are tabulated on Table 2.

3.3. Determination of the absorption coefficient and the optical band gap

The absorption coefficient, α of different thickness of CdTe thin film is calculated from the experimental data of transmittance (T) and reflectance (R) in strong absorption region using the relation [42]:

$$\alpha = \frac{1}{d} \ln\left[\frac{(1-R)^2 + [(1-R)^4 + 4R^2T^2]^{1/2}}{2T}\right] \tag{9}$$

where d is the sample thickness. Fig. 6 shows dependence of the absorption coefficient $\alpha(h\upsilon)$ on photon energy as a function of film thickness for CdTe thin films. It is known that pure semiconducting compounds have a sharp absorption edge (corresponding to forbidden energy bandgap) [43–47].

Fig. 6 shows the dependence of the absorption coefficient, α, on photon energy ($h\upsilon$) for polycrystalline CdTe thin films. In Fig. 6, it is clearly observed that the value of the absorption edge increases with increasing the film thickness.

The shapes of absorption spectra for CdTe thin films Show that the respective films have a stoichiometric composition. In order to complete the calculation of the optical constants, the extinction coefficient is estimated from the values of α and λ using the known formula $k=\alpha\lambda/4\pi$. Fig. 7 illustrates the dependence of k on wavelength for different samples of thin films. It is known, that in the vicinity of the fundamental absorption edge, for allowed direct band-to-band transitions, neglecting exciton effects, the absorption coefficient is described by the

$$\alpha(h\upsilon)=\frac{K(h\upsilon-E_g^{opt})^m}{h\upsilon}, \quad (10)$$

where K is a characteristic parameter (independent of photon energy) for respective transitions [48], $h\upsilon$ denotes photon energy, E_g^{opt} is optical energy gap and m is a number which characterizes the transition process. Different authors [40–42,49–51] have suggested different values of m for different glasses, $m=2$ for most amorphous semiconductors (indirect transition) and $m=1/2$ for most of crystalline semiconductor (direct transition). In the case of different thickness of polycrystalline of CdTe thin films the direct and are valid. For higher values ($\alpha \geq 10^4$ cm^{-1}) the absorption coefficient, α (where the absorption is associated with interband transitions), the energy gap can be determined. Fig. 8 is a typical best fit of and $(\alpha h\upsilon)^2$ vs. photon energy ($h\upsilon$) for different thickness of CdTe thin films. The values of the direct optical band gap E_g^{opt} were taken as the intercept of $(\alpha h\upsilon)^2$ vs. ($h\upsilon$) at $(\alpha h\upsilon)^2=0$ for the allowed direct transition. The direct optical band gap derived for each film is listed in Table 2. The optical band gap increases with increasing the film thickness, which may be attributing to the increase in crystallites size. The increase of crystallites size with increasing the film thickness may be attributed to the decrease in the FWHM at each reflection and also may be interpreted in terms of a columnar grain growth in the structure, which improves the crystallinity of the film [52]. The improvement in crystallinity is owing to an increase in the ability of add atoms to move towards stable sites in the lattice. Thicker films are characterized by more homogeneous network, which minimizes the number of defects and localized states, and thus the optical band gap increases [53,54].

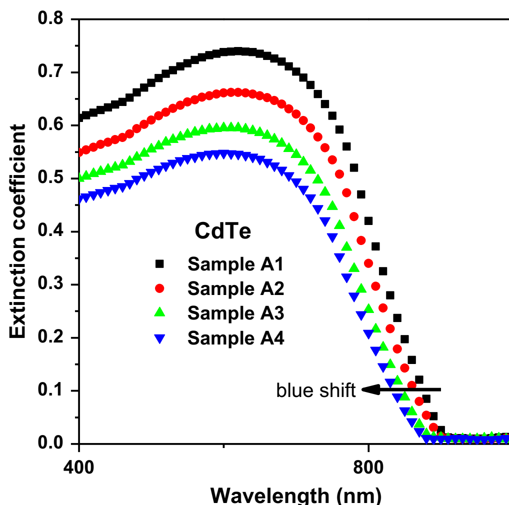

Fig. 7. Plotting of Extinction coefficient as a function of wavelengths energy of CdTe films/flexible substrates of different thicknesses.

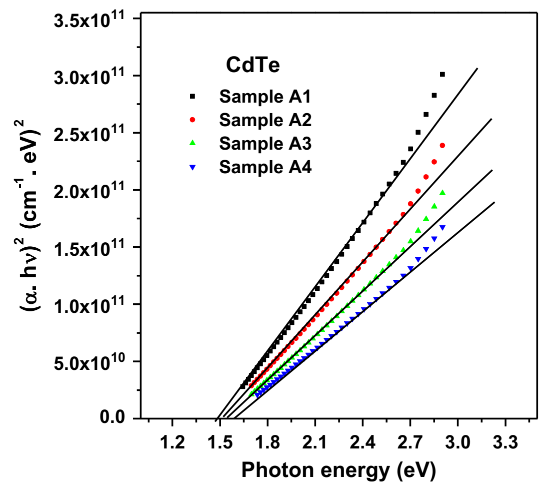

Fig. 8. Plotting of $(\alpha h\upsilon)^2$ as a function of wavelengths energy of CdTe films/flexible substrates of different thicknesses.

4. Conclusion

CdTe thin films of different thicknesses were deposited onto flexible polymer substrates by using the thermal evaporation technique. The calculated crystallite size for the studied CdTe/flexible substrates showed a nanostructure and the crystallite size increases with increasing of the film thickness. The calculated microstrain decreases with the increase of the film thickness which can be interpreted by the decrease in the concentration of lattice imperfections. Optical constants as the refractive index (n) and the extinction coefficient (k) were calculated on the basis of Swanepoel's method using the measured transmittance at normal incidence. The increase in refractive index with increasing film thickness may be attributed to the increased density of the film and increase in crystallites size. The single oscillator parameters E_o, E_d were calculated by applying the Wemple–DiDomenico (WDD) model. The calculated optical band gaps increase with increasing the film thickness and the transition were direct optical transitions. The increase of E_g^{opt} may be attributing to the increase in crystallites size. The increase of grain size with thickness can be attributed to the improved crystallinity of the film because thicker films are characterized by more homogeneous network, which minimizes the number of defects and localized states, and thus the optical band gap increases.

References

[1] X. Mathew, G.W. Thomson, V.P. Singh, J.C. McClure, S. Velumani, N. R. Mathews, P.J. Sebastian, Sol. Energy Mater. Sol. Cells 76 (2003) 293.
[2] K.L. Chopra, S.R. Das, Thin Film Solar Cells, Plenum Press, New York, 1983.

[3] G.P. Hernandez, X. Mathew, J.P. Enriquez, N.R. Mathews, P.J. Sebastian, Sol. Energy Mater. Sol. Cells 70 (2001) 269.
[4] M.G. Peters, A.L. Fahrenbruch, R.H. Bube, J. Vac. Sci. Technol. A 6 (1988) 3098.
[5] S. Sen, H. Konkel, S.J. Tight, L.G. Bland, S.R. Sharma, R.E. Taylor, J. Cryst. Growth 86 (1988) 111.
[6] N.B. Chaure, A.P. Samantilleke, I.M. Dharmadasa, Sol. Energy Mater. Sol. Cells 77 (2003) 303.
[7] D.J. Flood, W. Irving, Advanced solar cells for satellite power systems, NASA Technical Memorandum 106777, November, 1994.
[8] J.C. McClure, V.P. Singh, G.B. Lush, E. Clark, G. Thompson, Sol. Energy Mater. Sol. Cells 55 (1998) 141.
[9] I.M. Dharmadasa, A.P. Samantilleke, N.B. Chaure, J. Young, Semicond. Sci. Technol. 17 (2002) 1238.
[10] A. Carlos, P.J. Sebastian, O. Solorza, S.A. Gamboa, Adv. Mater. Opt. Electron. 7 (1997) 29.
[11] V.P. Singh, G.B. Lush, R. Santiesteban, J.C. McClure, H. Chavez, American Institute of Physics Conference Proceedings, No. 325, 1995, p. 235.
[12] H. Chavez, R. Santiesteban, J.C. McClure, V.P. Singh, J. Mater. Sci. Mater. Electron. 6 (1995) 21.
[13] R.K. Pandey, S. Maffi, L.P. Bicelli, Mater. Chem. Phys. 37 (1994) 141.
[14] A.E. Rakhshani, Y. Makdisi, X. Mathew, N.R. Mathews, Phys. Stat. Sol. A 168 (1998) 177.
[15] A.E. Rakhshani, J. Appl. Phys. 81 (1997) 7988.
[16] X. Mathew, P.J. Sebastian, Sol. Energy Mater. Sol. Cells 59 (1999) 85.
[17] X. Mathew, P.J. Sebastian, A. Sanchez, J. Campos, Sol. Energy Mater. Sol. Cells 59 (1999) 99.
[18] X. Mathew, J.P. Enriquez, Sol. Energy Mater. Sol. Cells 63 (2000) 347.
[19] A.E. Rakhshani, H.A. Ramazaniyan, Phys. Stat. Sol. A 172 (1999) 379.
[20] X. Mathew, J. Phys. D: Appl. Phys. 33 (2000) 1565.
[21] A.E. Rakhshani, Phys. Stat. Sol. A 169 (1998) 85.
[22] A.E. Rakhshani, J. Phys.: Condens. Matter 11 (1999) 9115.
[23] A. Seth, G.B. Lush, J.C. McClure, V.P. Singh, D. Flood, Sol. Energy Mater. Sol. Cells 59 (1999) 35.
[24] M.E. Calixto, J.C. McClure, V.P. Singh, A. Bronson, P.J. Sebastian, X. Mathew, Sol. Energy Mater. Sol. Cells 63 (2000) 325.
[25] A.E. Rakhshani, Y. Makdisi, Phys. Stat. Sol. A 179 (2000) 159.
[26] E.R. Shaaban, Ishu Kansal, José M.F. Ferreira, Physica B: Condensed matter 404 (2009) 3571.
[27] X. Mathew, J.R. Arizmendi, J. Campos, P.J. Sebastian, N.R. Mathews, C. R. Jimenez, M.G. Jimenez, R. Silva-Gonzalez, M.E. Hernandez-Torres, R. Dhere, Sol. Energy Mater. Sol. Cells 70 (2001) 379.
[28] G.P. Hernandez, X. Mathew, J.P. Enriquez, N.R. Mathews, P.J. Sebastian, Sol. Energy Mater. Sol. Cells 70 (2001) 269.
[29] G. Maurin, O. Solorza, H. Takenouti, J. Electroanal. Chem. 202 (1986) 323.
[30] J. Touskova, D. Kindl, J. Tousek, Sol. Energy Mater. 18 (1989) 377.
[31] S. Moorthy Babu, R. Dhanasekaran, P. Ramasamy, Thin Solid Films 202 (1991) 67.
[32] ⟨http://www.professionalplastics.com/professionalplastics/Thermal Properties Of Plastic Materials.pdf⟩.
[33] K. Kamide, M. Saito, Polym. J. 17 (1985) 19.
[34] E.R. Shaaban, N. Afify, A. El-Taher, J. Alloys Compd. 482 (2009) 400.
[35] A.K. Kulkarni, K.H. Schulz, T.S. Lima, M. Khanb, Thin Solid Films 308–309 (1997) 1.
[36] L.E. Brus, J. Chem. Phys. 80 (1984) 4403.
[37] R. Swanepoel R, J. Phys. E: Sci. Instrum. 17 (1984) 896.
[38] E. Márquez, J.M. González-Leal, A.M. Bernal-Oliva, R. Jiménez-Garay, T. Wagner, J. Non-Cryst. Solids 354 (2008) 503.
[39] E.R. Shaaban, M.A. Kaid, E.S. Moustafa, A. Adel, J. Phys. D: Appl. Phys. 41 (2008) 125301.
[40] E.R. Shaaban, Philos. Mag. 88 (2008) 781.
[41] S.H. Wemple, M. DiDomenico, Phys. Rev. B 3 (1971) 1338.
[42] M. Kastner, Phys. Rev. Lett. 28 (1972) 355.
[43] L.L. Kazmersky (Ed.), Polycrystalline and Amorphous Thin Films and Devices, Academic Press, New York, 1980.
[44] R. Swanepoel, J. Phys. E: Sci. Instrum. 16 (1983) 121; R. Swanepoel, J. Phys. E: Sci. Instrum. 17 (1984) 896.
[45] E. Marques, J.B. Ramerez-Malo, P. Villares, R. Jimenez-Garay, R. Swanepoel, Thin Solid Films 254 (1995) 83.
[46] C. Baban, G.I. Rusu, Appl. Surf. Sci. 211 (2003) 6.
[47] M. Nowak, Thin Solid Films 266 (1995) 258.
[48] J.I. Pankove, Optical Processes in Semiconductors, Dover, New York, 1971, 44.
[49] E.A. Davis, N.F. Mott, Philos. Mag. 22 (1970) 903.
[50] E.A. Fagen, H. Fritzsche, J. Non-Cryst. Solids 2 (1970) 180.
[51] E.R. Shaaban, M. Abdel-Rahman, El Sayed Yousef, M.T. Dessouky, Thin Solid Films 515 (2007) 3810.
[52] Mustafa Öztas, Metin Bedir, Thin Solid Films 516 (2008) 1703.
[53] S.K. Biswas, S. Chaudhuri, A. Choudhury, Phys. Status Solidi A 105 (1988) 467.
[54] K.I. Arshak, C. Ahogarth, Thin Solid Films 137 (1986) 281.